NASA TECHNICAL MEMORANDUM

NASA TM X-1428

NASA TM X-1428

EXPERIMENTAL RESULTS OF HEAT TRANSFER AND PRESSURE DROP OF ARGON FLOWING THROUGH SINGLE TUBE WITH INTERNAL INTERRUPTED FINS

by David Namkoong and Michael P. Lynch

Lewis Research Center

Cleveland, Ohio

NATIONAL AERONAUTICS AND SPACE ADMINISTRATION • WASHINGTON, D. C. • AUGUST 1967

NASA TM X-1428

EXPERIMENTAL RESULTS OF HEAT TRANSFER AND PRESSURE DROP OF ARGON FLOWING THROUGH SINGLE TUBE WITH INTERNAL INTERRUPTED FINS

By David Namkoong and Michael P. Lynch

Lewis Research Center
Cleveland, Ohio

NATIONAL AERONAUTICS AND SPACE ADMINISTRATION

For sale by the Clearinghouse for Federal Scientific and Technical Information
Springfield, Virginia 22151 – CFSTI price $3.00

EXPERIMENTAL RESULTS OF HEAT TRANSFER AND PRESSURE DROP OF ARGON FLOWING THROUGH SINGLE TUBE WITH INTERNAL INTERRUPTED FINS

by David Namkoong and Michael P. Lynch

Lewis Research Center

SUMMARY

A $1\frac{1}{4}$-inch (3.18 cm) tube with internal, interrupted fins was tested with argon. Friction factors were calculated from data with and without heat addition. Values of the heat-transfer parameter $N_{St}N_{Pr}^{2/3}$ were also obtained, where N_{St} is the Stanton number and N_{Pr} is the Prandtl number. Plotted against Reynolds number up to 2200, the friction factor and the heat-transfer parameter curves were similar to those of a louvered plate-fin geometry with the same interrupted fin length.

INTRODUCTION

To increase the transfer of heat, extended surfaces are used in many applications and vary widely in their design. Among the most common types of extended surface are fins on the outside surfaces of tubes (such as on evaporators and condensers) and continuous and louvered fins in compact, flat-plate heat exchangers. Recent designs in space-power-conversion systems indicate, however, that internal finning of tubes can be used to advantage. Reference 1 indicates that the size of gas radiators can be reduced within performance limits by a proper choice of internal finning. Another application of internal finning is in that portion of a Brayton cycle system, the receiver, where the gas absorbs the primary heat.

In current considerations of a Brayton cycle system, heat is to be transferred to argon under a stringent pressure drop requirement within an established geometry of the heat receiver. A preliminary analysis indicated that a continuous extended surface within each tube would not be adequate and that only by staggering the extended surface, thereby continually interrupting the boundary layer, would the requirements be approached. It was evident almost immediately, however, that data pertinent to internal, interrupted finning of tubes were virtually nonexistent. One reference that includes this type of finning in its heat-transfer and pressure loss study is that of Hilding and Coogan (ref. 2).

The range of Reynolds number and the axial lengths of fins used in their experiments, however, were beyond the range of interest of this report. To obtain pertinent data, a single-tube test program was initiated. The internal, interrupted fin design was based on louvered plate-fin data (ref. 3), where the fin length in the direction of flow was 3/4 inch (1.90 cm). The internal finning of the tube consisted of six radial fins forming a three-petal rosette, 3/4-inch (1.90 cm) in the flow direction. Every other rosette was rotated 30° to interrupt the boundary layer buildup. The results of this test program were compared with the louvered plate-fin surface on which it was based.

SYMBOLS

A	effective heat-transfer area
c_p	specific heat of argon
D_e	equivalent diameter
f	friction factor
G	flow rate per unit cross-sectional area
g	gravitational constant
h	convective heat-transfer coefficient
LMTD	log mean temperature difference
l	length of finned section of tube
N_{Pr}	Prandtl number
N_{Re}	Reynolds number
N_{St}	Stanton number
P	pressure
ΔP	pressure drop
P'	effective perimeter
T	temperature
ΔT	temperature difference
W	flow rate
x	distance along tube length
z	height of water
ρ	gas density

Subscripts:

Ar	argon
a	acceleration
av	average
f	friction
m	measured
p	plenum
w	wall
0	location immediately upstream of rotameter
1	gas inlet
2	gas discharge
10, 20, 30, 40, 50	locations of tube wall along its length
60, 61	location at gas discharge

APPARATUS AND PROCEDURE

A schematic diagram of the experimental system is shown in figure 1. Argon was supplied from a pressurized bottle. Flow passed through a coarse regulator and, further downstream, through a fine-adjusting regulator. The flow rate was measured by a rotameter. Flow passed into a plenum chamber and then into an entry tube of the same inner diameter as the test section. The flow continued past the flanged joint into the test section. Following the test section, the argon passed into a U-tube section in an insulated enclosure. Two coarse screens in series were inserted into this section to provide a measurement of the bulk stream temperature of the argon. The 180° bend in the tube in this section provided for a return tube. The exhaust valve was installed to provide the capability for pressurization as well as a means to test for leaks. Figure 2 shows the components set up for a cold-flow test.

For the heat-transfer experiments, the test section was submerged in a salt bath - a mixture of sodium nitrite, potassium nitrate, and sodium nitrate. The entry section was wound with 1/4-inch (0.64 cm) copper tubing. Water flowing through the copper tube cooled this entry section and minimized the transfer of heat from the tube wall to the argon.

The test section was a single tube with an inner diameter of 1.20 inches (3.0 cm) and with a finned length of 36 inches (91.5 cm). The tube and the internal fins are shown separately in figure 3. The finning arrangement as shown is an initial design where the rosettes were welded to a 1/4-inch (0.64 cm) tube. Every rosette was rotated 30° in one direction from the previous rosette. The small, dimplelike depressions on the fins provided a location for slugs of braze material. Insertion of the finned section into the tube was difficult, and the results after the braze operation indicated that many of the rosettes were distorted during insertion. The subsequent arrangement of the rosette-type fins, 0.005 inch (0.013 cm) in thickness, is shown in figure 4. The 1/4-inch (0.64 cm) tube was eliminated, and the fins were staggered so that only every other rosette was rotated 30° in one direction. Instead of slugs of braze material, foillike braze was inserted between the rosettes and the tube wall. This method of braze eliminated the need for depressions in the rosettes. Radiographs after the braze operation indicated good contact of the rosettes to the tube wall and no distortion of the fins.

The tests were conducted under conditions without heat transfer (cold flow test) and with heat transfer. Tests without heat transfer provided data for cold-flow friction factors. Tests with heat transfer provided data for the heat-transfer parameter $N_{St}N_{Pr}^{2/3}$ as well as for friction factors. In the heat-transfer tests, shop air was used to achieve a near-steady-state condition. When this condition was reached, shop air was closed off, and argon was allowed to run through the system. When steady state was reached with argon, a datum point was recorded. This procedure was followed before each datum point in early tests but was later used for only the first of a series of data points.

INSTRUMENTATION

The design parameters to be monitored in the tests required instrumentation to measure temperature, pressure, and flow rate.

Wall and stream temperatures were measured by iron-constantan, type J, stainless-steel sheathed thermocouples. The junctions on the wall or surface thermocouples were of the open type that were sealed in cement to protect them from the corrosive effect of the salt solution.

The temperature ranged from 50° to 400° F (283° to 478° K) and was indicated on a self-balancing potentiometer. Since the indicator was a single-dial type, the thermocouples were connected manually to a multipoint switch. The temperatures were read directly on the circular indicator chart that ranged from 0° to 400° F (255° to 478° K) in 1° F (0.56° K) increments. The readings then were recorded by hand to prepared data forms.

Pressure was measured by Bourdon-tube-type gages and a manometer for differential pressure readings. Since some differential pressure readings of less than 1 inch (2.5 cm) of water were expected, a water micromanometer was utilized. This instrument incorporated a water reservoir that was motor driven in a vertical direction. Under the conditions of the test, the reservoir was driven vertically so that the water level returned to a reference mark. The sensitivity of the instrument was increased by positioning the viewing portion of the manometer to 5° from the horizontal. The vertical distance traveled, which was read on a dial indicator, was the pressure difference measurement in terms of inches of water. The accuracy of the readings was determined by the degree of repeatability at a no-flow condition. During the initial stages of the test (the cold-flow runs) the instrument was read within ±0.010 inch (0.025 cm) of water. In the latter stages of testing, the manometer was read within ±0.005 inch (0.013 cm) of water.

Argon flow rate was measured by a rotameter with a stainless-steel guided float. The rotameter was calibrated by a positive-displacement wet-test meter that was accurate to 1 percent of the flow rate. The instrument was calibrated with argon at about the same conditions of temperature and pressure as experienced in the test. The capacity of the rotameter was 28.0 pounds per hour (1270 kg/hr) of argon. The rotameter had a maximum reading of 600, which could be read within an accuracy of ±10 units on the calibration curve. In terms of flow rate, the accuracy in reading the rotameter plus the accuracy of calibration resulted in a possible error of ±0.5 pound per hour (22.6 kg/hr).

METHOD OF ANALYSIS

The data were reduced to parameters generally used in frictional pressure drop and heat-transfer calculations.

The frictional pressure drop was the result of subtracting the pressure change due to the change in momentum (from heat addition) from the measured pressure difference. In equation form,

$$\Delta P_f = \Delta P_m - \Delta P_a$$

$$= \Delta P_m - \frac{G^2}{g}\left(\frac{1}{\rho_2} - \frac{1}{\rho_1}\right)$$

The friction factor f was calculated as follows:

$$\Delta P_f = 4f \frac{l}{D_e} \frac{G^2}{\rho 2g}$$

$$f = \frac{2gD_e}{4l} \frac{\rho \, \Delta P_f}{G^2}$$

The density ρ, used in calculating f, was obtained at the log mean gas temperature.

The parameter used extensively in heat-exchanger calculations is

$$\frac{h}{Gc_p}(N_{Pr})^{2/3} \equiv N_{St}N_{Pr}^{2/3}$$

If it is assumed that the salt side of the tube operates at $h = \infty$ and that the gas side operates at a constant h, then the heat transferred to the gas is related to the temperature rise of the gas by

$$hA(LMTD) = Wc_p \, \Delta T$$

The temperature distribution is illustrated in sketch (a):

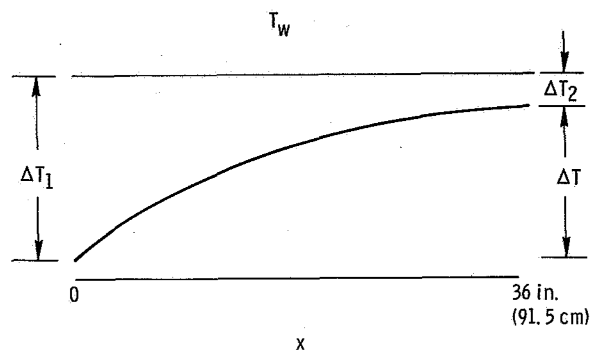

(a)

In this case, then,

$$\Delta T = \Delta T_1 - \Delta T_2$$

The log mean temperature difference LMTD is defined as

$$LMTD \equiv \frac{\Delta T_1 - \Delta T_2}{\ln \frac{\Delta T_1}{\Delta T_2}} = \frac{\Delta T}{\ln \frac{\Delta T_1}{\Delta T_2}}$$

The heat-transfer area A is equal to the effective perimeter P' at a typical gas-flow passage cross section multiplied by the length over which the measurement is taken. Substituting these terms into the basic equation results in

$$hP'l \frac{\Delta T}{\ln \frac{\Delta T_1}{\Delta T_2}} = Wc_p \Delta T$$

Rearranging yields

$$\frac{h}{Wc_p} = \frac{\ln \frac{\Delta T_1}{\Delta T_2}}{P'l}$$

Substituting into the generalized parameter gives

$$\frac{h}{Gc_p} (N_{Pr})^{2/3} = \frac{A(N_{Pr})^{2/3}}{P'l} \ln \frac{\Delta T_1}{\Delta T_2}$$

$$N_{St}N_{Pr}^{2/3} = \frac{A(N_{Pr})^{2/3}}{P'l} \ln \frac{\Delta T_1}{\Delta T_2}$$

For a given geometry and an essentially constant value of $(N_{Pr})^{2/3}$, the term $A(N_{Pr})^{2/3}/l$ is constant. The range of values of P' depends on the fin effectiveness, which, for the conditions covered, varies little. It may be claimed, therefore, that $N_{St}N_{Pr}^{2/3}$ is primarily determined by $\ln(\Delta T_1/\Delta T_2)$.

Predicting the friction factor and the heat-transfer parameter $N_{St}N_{Pr}^{2/3}$ as a function of Reynolds number presented a dilemma since there were virtually no data available on interrupted fins within a tube. It was decided, therefore, to study interrupted (louvered) fins on plate-fin surfaces to ascertain the more significant factors in heat transfer and pressure drop. Comparisons based on equivalent diameter, length-diameter ratio, fin height, and fin length indicated that the most significant factor was fin length. Curves of a louvered plate-fin surface with the same length of interrupted fins as that under investigation (3/4-in. or 1.90 cm in the direction of flow designated 3/4 (b) - 11.1 in ref. 2) are included in the RESULTS section for comparison.

RESULTS

Argon flow through an internal, interrupted finned tube was investigated to obtain heat-transfer data and frictional pressure-drop data with and without heat addition. Argon flow rate was varied to establish a range of Reynolds number values. The Reynolds number was based on the cross-sectional dimensions of the tube and fins. The following is a discussion of the results.

Friction Factor

Values of friction factor were calculated from pressure-drop data with and without heat addition. The data and calculated results are presented in table I for the cold-flow pressure-drop tests and in table II for heat-transfer and pressure-drop tests with heat addition. For the range of Reynolds number investigated, the measured pressure drop ranged from a maximum of 0.357 inch (0.90 cm) to a minimum of 0.019 inch (0.048 cm) of water. The frictional pressure drop ranged correspondingly from 0.01177 to 0.000686 psi (81 to 4.7 N/sq m). All the pressure-drop results are shown in figure 5 in terms of the friction factor as a function of Reynolds number. There is no difference between cold flow and heat addition with regard to fairing a single curve through the data points. The scatter of data was due to the experimental errors in reading the micromanometer, in reading the rotameter, and in calibrating the rotameter, as mentioned in the INSTRUMENTATION discussion. Virtually all the data points, however, fall within 10 percent of the data curve.

The reference curve is that of a louvered plate-fin surface with interrupted fins measuring 3/4 inch (1.90 cm) in the direction of flow. Comparison of the data curve with the reference curve shows not only a similar shape but virtually an identical average slope. The maximum displacement between the curves is approximately 10 percent over the range of Reynolds number investigated.

Heat Transfer

Tests with heat addition were conducted with the bulk of the salt bath initially at about 345° F (447° K) or 25° F (14° K) above its freezing temperature (320° F or 433° K). The temperature variation of the bath of this no-flow condition is presented in table II, run 10. Thermocouples on the tube surface indicated a uniform temperature along the test section except for T_{10}. This thermocouple, located about 1 inch ($2\frac{1}{2}$ cm) below the bath surface, was below the freezing temperature of the salt. This measurement was substantiated by solid (frozen) salt forming around the tube. Temperatures at the bottom of the salt bath, measured as T_{60} and T_{61}, indicated a slightly lower temperature than that of the bulk of the bath. With flow, all the wall temperatures fell within a short time interval, most of them below the freezing point.

Further tests were conducted with higher bath temperatures to minimize the formation of frozen salt. The no-flow condition at a higher salt temperature is tabulated as run 11 in table II. Though the wall thermocouples at two stations along the tube became inoperative, the remaining thermocouples indicated that all the tube was appreciably above the salt freezing temperature. The temperature readings were substantiated by a lack of frozen salt around the tube. Again the upper thermocouple T_{10} indicated a lower temperature than that of the bulk of the bath (about 23^{o} F or 13^{o} K in this case). The lower part of the bath also indicated temperatures below the bath temperature; T_{60} and T_{61} indicated about 19^{o} F or 11^{o} K cooler.

Since it was noted that the points based on data at the higher Reynolds number have the same trend as the reference curve and, further, that the friction-factor-data curve was very similar to the reference curve, a curve was drawn through the data points such as the one shown (fig. 5). This curve fits the points well at the higher Reynolds numbers and is displaced from the reference curve by about 15 percent. There is a wide discrepancy at the lower Reynolds numbers, however. The two or three data points involved occur at the lowest flow rates. This suggests that at the low flow rates, conductive heat losses at the bottom of the salt bath exerted a greater influence than the convective heat transfer.

SUMMARY OF RESULTS

Values of friction factor and $N_{St}N_{Pr}^{2/3}$ of argon flowing through a single tube with internal, interrupted fins were plotted as a function of Reynolds number (where N_{St} is the Stanton number and N_{Pr} is the Prandtl number). Curves faired through the data points were compared with those of a louvered plate-fin geometry. The following results were obtained:

1. The average slope of the friction factor curve was virtually identical to that of the louvered plate-fin geometry. The faired curve was up to approximately 10 percent lower than that of the louvered plate-fin over the range of Reynolds numbers from 350 to 2200.

2. A curve similar to the heat-transfer parameter curve $N_{St}N_{Pr}^{2/3}$ of a louvered plate-fin geometry could be faired through the data points over the range of Reynolds number from 800 to 1900. This curve was approximately 15 percent lower than the reference curve.

Lewis Research Center,
National Aeronautics and Space Administration,
Cleveland, Ohio, April 20, 1967,
120-33-07-03-22.

REFERENCES

1. Lieblein, Seymour: Heat-Transfer Aspects of Space Radiators. Paper presented at the AIChE and ASME 6th National Heat Transfer Conference, Boston, Aug. 11-14, 1963.
2. Hilding, Winthrop, E.; and Coogan, Charles H., Jr.: Heat Transfer and Pressure Loss Measurements in Internally Finned Tubes. Symposium on Air-Cooled Heat Exchangers, 7th National Heat Transfer Conference, Cleveland, Aug. 10, 1964. ASME, 1964, pp. 57-85.
3. Kays, W. M.; and London, A. L.: Compact Heat Exchangers. Second ed., McGraw-Hill Book Co., Inc., 1964.

TABLE I. - COLD-FLOW PRESSURE-DROP TESTS

(a) U.S. Customary Units

Test	Upstream pressure, P_0, psi	Plenum pressure, P_{pl}, psi	Measured pressure drop, ΔP_m, psi	Flow rate, W, lb/hr	Upstream temperature, T_0, ^oR	Reynolds number, N_{Re}	Gas density, ρ, lb/cu ft	Water height, z, in.	Friction factor, f
1	15.5	15.25	0.00213	10.03	517	876	0.1099	0.059	0.0445
2	15.55	15.0	.00643	24.1	517	2105	.1080	.178	.023
3	15.5	15.1	.00444	18.04	517	1578	.1088	.123	.0285
4	14.45	14.2	.000686	5.20	525	454	.1018	.019	.0495
5	14.45	14.2	.001662	9.30	524	810	.1018	.046	.0376
6	14.5	14.2	.002925	13.43	523	1172	.1018	.081	.0315
7	14.7	14.2	.00445	18.05	523	1575	.1018	.123	.0268
8	14.82	14.2	.00619	22.8	523	1990	.1018	.171	.0232
9	14.95	14.2	.00698	25.0	522	2180	.1018	.193	.0218

(b) International System of Units

Test	Upstream pressure, P_0, N/sq m	Plenum pressure, P_{pl}, N/sq m	Measured pressure drop, ΔP_m, N/sq m	Flow rate, W, kg/hr	Upstream temperature, T_0, ^oK	Reynolds number, N_{Re}	Gas density, ρ, kg/cu m	Water height, z, cm	Friction factor, f
1	107 000	105 000	14.7	4.55	287	876	1.76	0.150	0.0445
2	107 000	103 000	44.3	10.93	287	2105	1.73	.452	.023
3	107 000	105 000	30.6	8.19	287	1578	1.74	.312	.0285
4	99 500	98 000	47.3	2.36	292	454	1.63	.048	.0495
5	99 500	98 000	11.5	4.22	291	810	1.63	.117	.0376
6	100 000	98 000	20.1	6.10	291	1172	1.63	.206	.0315
7	101 000	98 000	30.7	8.19	291	1575	1.63	.312	.0268
8	102 000	98 000	42.6	10.34	291	1990	1.63	.434	.0232
9	103 000	98 000	48.1	11.34	290	2180	1.63	.490	.0218

TABLE II. - HEAT-TRANSFER AND PRESSURE-DROP TESTS WITH HEAT ADDITION

(a) Standard U.S. Customary Units

Test	Upstream pressure, P_0, psia	Plenum pressure, P_{pl}, psia	Flow rate, W, lb/hr	Upstream temperature, T_0, °R	Gas inlet temperature, T_1, °F	Tube wall temperature, °F: T_{10}	T_{20}	T_{30}	T_{40}	T_{50}	Gas discharge temperature, °F: T_{60}	T_{61}	Temperature difference, °F: Inlet, ΔT_1	Discharge, ΔT_2	Heat-transfer parameter, $N_{St}N_{Pr}^{2/3}$	Reynolds number, N_{Re}	Gas density, kg/m: Average	Discharge	Inlet	Water height, z, in.	Pressure drop, ΔP, psi: Measured, ΔP_m	Acceleration, ΔP_a	Friction, ΔP_f	Friction factor, f
10	-----	-----	0	---	---	304	345	345	344	343	337	337	---	---	-------	----	------	------	------	-----	--------	--------	--------	------
11	-----	-----	0	---	---	366	---	---	389	386	370	370	---	---	-------	----	------	------	------	-----	--------	--------	--------	------
12	15.51	14.41	27.25	510	83	334	---	---	376	382	356	356	251	26	0.00633	1820	0.0789	0.0656	0.0987	0.344	0.01242	0.00115	0.01127	0.0229
13	15.16	14.41	20.65	528	83	330	---	---	376	382	361	361	247	21	.00656	1350	.0786	.0654	.0987	.247	.00893	.00066	.00827	.0291
14	14.93	14.41	15.95	523	83	345	---	---	384	387	375	375	262	12	.00799	1040	.0779	.0642	.0987	.172	.00622	.00042	.00580	.0342
15	14.76	14.41	10.12	526	83	350	---	---	390	391	382	382	267	9	.00880	652	.0775	.0637	.0987	.098	.00354	.00017	.00337	.0488
16	14.64	14.41	5.18	530	84	352	---	---	394	391	384	384	268	7	.00923	361	.0772	.0635	.0987	.037	.001337	.00053	.001284	.0606
17	15.59	14.46	27.4	525	92	346	---	---	388	390	360	360	254	30	.00593	1890	.0785	.0656	.0975	.357	.01290	.00113	.01177	.0236
18	15.36	14.46	23.65	517	90	346	---	---	390	391	366	366	256	25	.00631	1630	.0782	.0651	.0979	.284	.01027	.00087	.00940	.0253
19	15.11	14.46	18.7	516	89	348	---	---	392	393	372	372	259	21	.00670	1290	.0779	.0647	.0980	.210	.00760	.00056	.00704	.0301
20	14.79	14.46	9.50	520	89	353	---	---	399	396	382	381	264	14	.00747	654	.0774	.0640	.0980	.081	.00293	.00015	.00278	.0460
21	14.98	14.46	15.8	531	89	346	---	---	389	394	380	380	257	14	.00777	1090	.0774	.0641	.0980	.163	.00590	.00041	.00549	.0326
22	14.93	14.46	13.62	528	91	351	---	---	392	396	383	383	260	13	.00788	940	.0772	.0638	.0979	.129	.00466	.00031	.00435	.0346
23	14.84	14.46	11.55	529	92	357	---	---	396	398	387	387	265	11	.00835	797	.0770	.0635	.0975	.097	.00351	.00022	.00329	.0355

(b) International System of Units

Test	Pressure, N/sq m: Upstream, P_0	Plenum, P_{pl}	Flow rate, W, kg/hr	Up stream temperature, T_0, °K	Gas inlet temperature, T_1, °K	Tube wall temperature, °K: T_{10}	T_{20}	T_{30}	T_{40}	T_{50}	Gas discharge temperature, °K: T_{60}	T_{61}	Temperature difference, °K: Inlet, ΔT_1	Discharge, ΔT_2	Heat-transfer parameter, $N_{St}N_{Pr}^{2/3}$	Reynolds number, N_{Re}	Gas density, kg/cu ft: Average	Discharge	Inlet	Water height, z, cm	Pressure drop, ΔP, N/sq m: Measured, ΔP_m	Acceleration, ΔP_a	Friction, ΔP_f	Friction factor, f
10	-------	------	0	---	---	425	447	447	446	466	443	443	---	--	-------	----	-----	-----	-----	-----	-----	----	-----	------
11	-------	------	0	---	---	459	---	---	471	470	461	461	---	--	-------	----	-----	-----	-----	-----	-----	----	-----	------
12	107 000	99 400	12.36	283	302	441	---	---	465	468	453	453	139	14	0.00633	1820	1.264	1.051	1.581	0.874	85.63	7.93	77.70	0.0229
13	104 000	99 400	9.37	293	302	439	---	---	465	468	456	456	137	12	.00656	1350	1.259	1.048	1.581	.627	61.57	4.55	57.02	.0291
14	103 000	99 400	7.23	290	302	447	---	---	469	471	464	464	146	7	.00799	1040	1.248	1.028	1.581	.437	42.89	2.90	39.99	.0342
15	102 000	99 400	4.59	292	302	450	---	---	472	473	468	468	148	5	.00880	652	1.241	1.020	1.581	.249	24.41	1.17	23.24	.0488
16	101 000	99 400	2.35	294	302	451	---	---	474	473	469	469	149	4	.00923	361	1.237	1.017	1.581	.094	9.22	.36	8.86	.0606
17	107 000	99 700	12.43	292	307	448	---	---	471	472	455	455	141	17	.00593	1890	1.257	1.051	1.562	.907	88.94	7.79	81.15	.0236
18	106 000	99 700	10.73	287	306	448	---	---	472	473	459	459	142	14	.00631	1630	1.253	1.043	1.568	.721	70.81	6.00	64.81	.0253
19	104 000	99 700	8.48	287	305	449	---	---	473	474	462	462	144	12	.00670	1290	1.248	1.036	1.570	.533	52.40	3.86	48.54	.0301
20	102 000	99 700	4.31	289	305	451	---	---	477	476	468	467	147	8	.00747	654	1.240	1.025	1.570	0.206	20.20	1.03	19.17	.0460
21	103 000	99 700	7.17	295	305	448	---	---	471	474	467	467	143	8	.00777	1090	1.240	1.027	1.570	.414	40.68	2.83	37.85	.0326
22	103 000	99 700	6.18	293	306	451	---	---	473	476	458	458	144	7	.00788	940	1.237	1.022	1.568	.328	32.13	2.14	29.99	.0346
23	102 000	99 700	5.24	294	307	454	---	---	476	477	471	471	147	6	.00835	797	1.233	1.017	1.562	.246	24.20	1.52	22.68	.0355

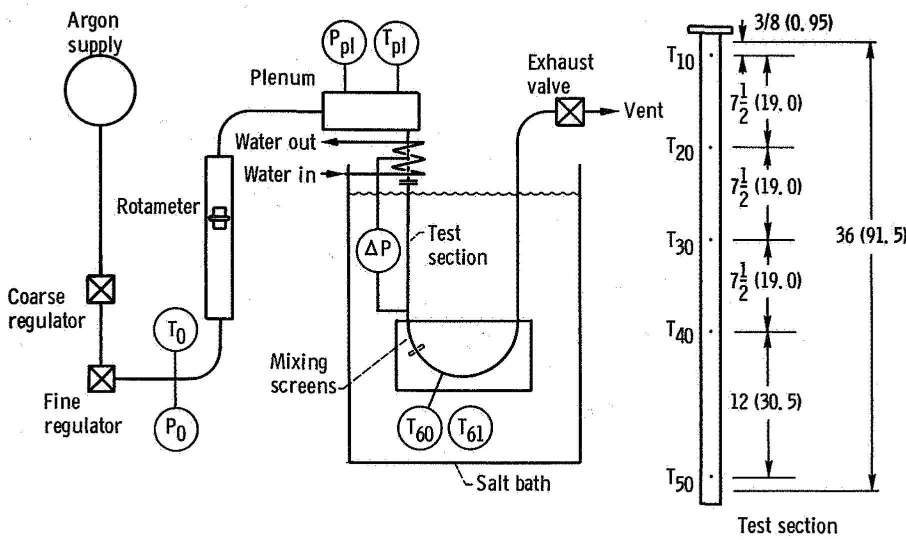

Figure 1. - Internal, interrupted finned tube test. All dimensions are in inches (cm).

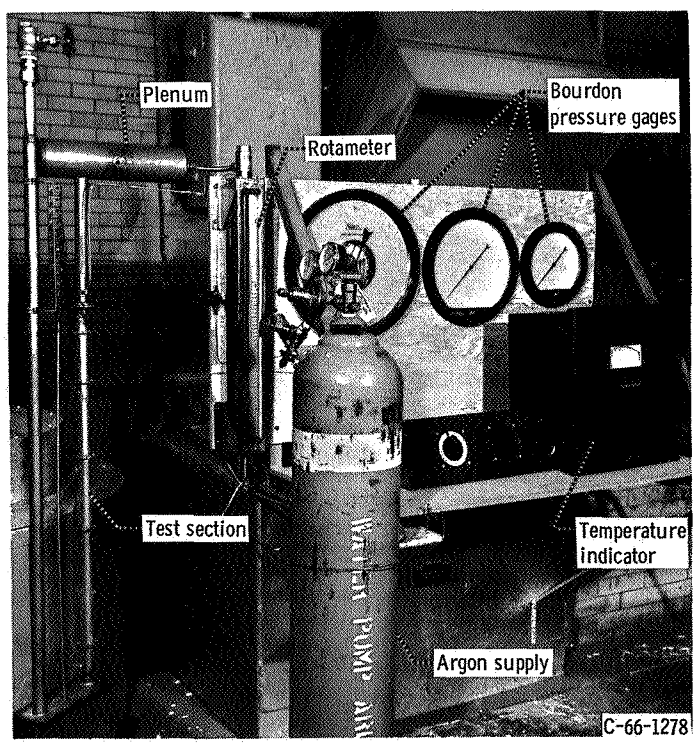

Figure 2. - Single tube with internal, interrupted fins for cold-flow test.

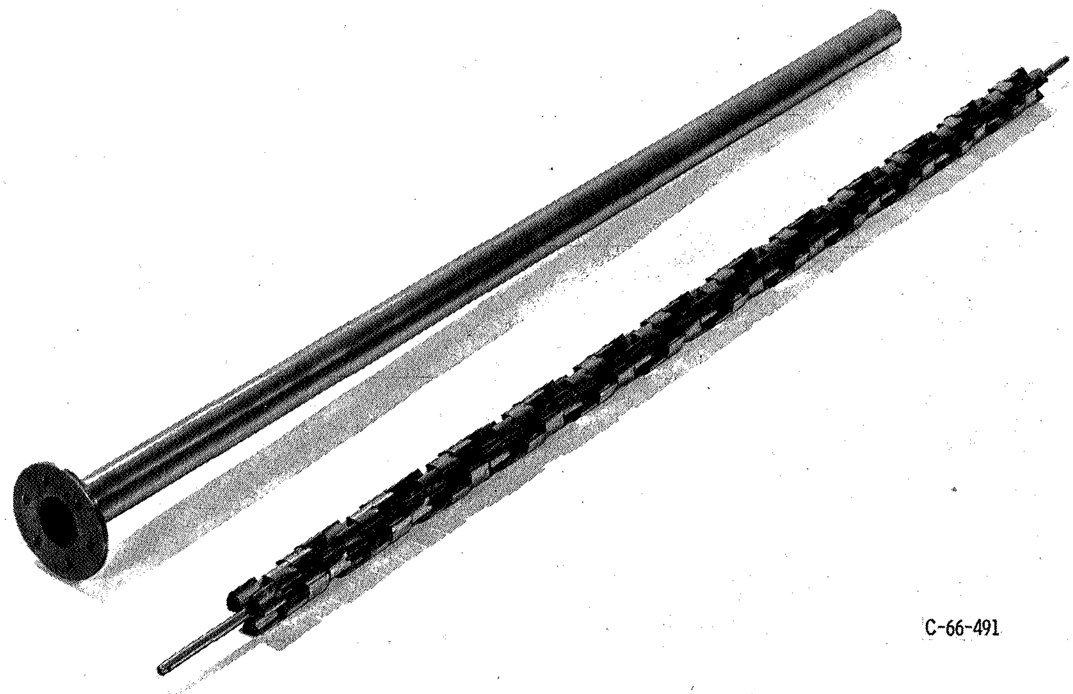

Figure 3. - Fins welded to 1/4-inch (0.64 cm) tube prior to insertion into flow tube.

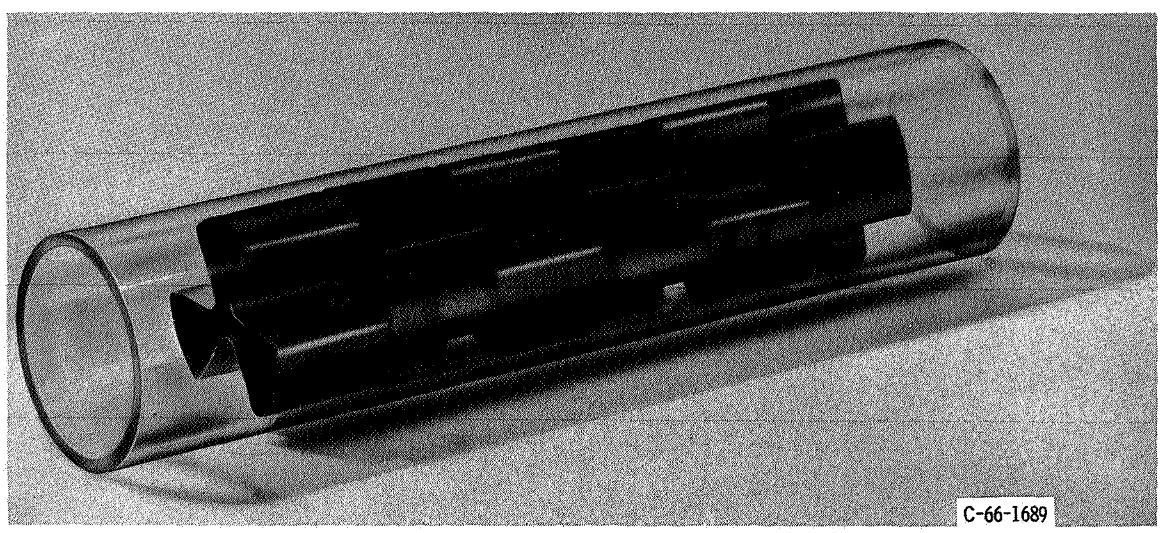

Figure 4. - Internal, rosette-type fins in interrupted flow pattern.

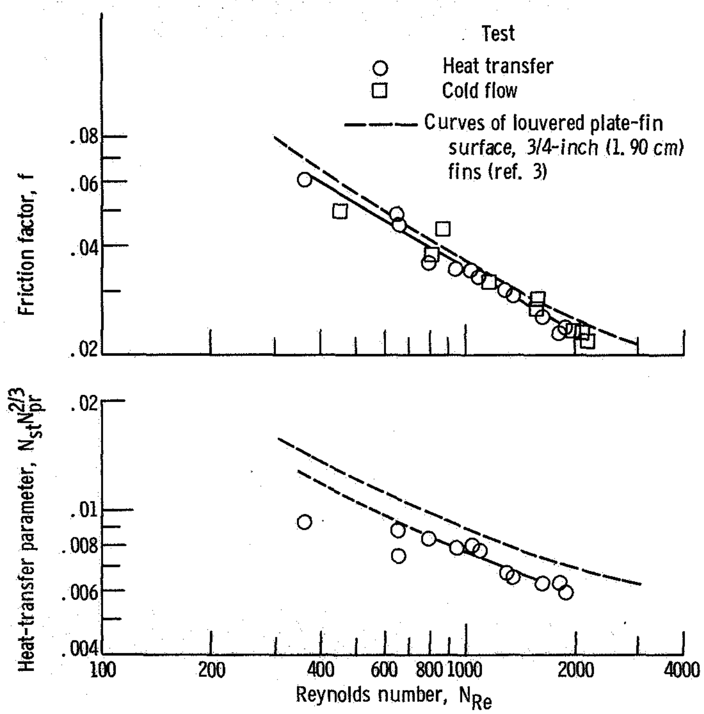

Figure 5. - Heat-transfer and friction factor characteristics of argon flow through internal, interrupted finned tube.